UNCERTAINTY QUANTIFICATION OF GRID REFINEMENT APPLIED TO THE FLUID DYNAMICS OF A HOLLOW FIBER MEMBRANE

Daniel Silveira Lira

daniel.lira@eq.ufcg.edu.br

Severino Rodrigues de Farias Neto

s.fariasn@gmail.com

Antonio Gilson Barbosa de Lima

antonio.gilson@ufcg.edu.br

UFCG

Rua Aprígio Veloso, 882, Bodocongó, CEP 58429-900, Campina Grande, Paraíba, Brazil

Abstract. *The GCI is an uncertainty estimation parameter based on the Richardson extrapolation developed with the objective to standardize and give more reliability to the results of grid convergence. In this work, the GCI was employed to evaluate the grid convergence of a systematically refined structured hexahedral grid, applied to model the laminar flow of fluid through a hollow fiber membrane using the resistance in series model in presence of concentration polarization. Three grids were produced, with respectively 1080, 10863 and 87759 elements. The model used in this study is an axisymmetric model of the flow through a membrane hollow fiber tube. For the solution of the Navier-Stokes equations, the Ansys CFX 15.0 package was used with a convergence criterion of* 10^{-6} *RMS. Results showed that the uncertainties of the fine grid solutions were within the acceptable range, achieving a maximum of 4.11% for the concentration polarization layer thickness variable. Therefore, the GCI can be regarded as a reliable method to assess grid convergence and quantify the uncertainties of grid refinement.*

Keywords: *Richardson Extrapolation, Convergence, Concentration Polarization.*

1 INTRODUCTION

The grid is a fundamental part in solving several physics and engineering problems which use complex boundary value problems of which solution is not very straightforward and therefore require the use of numerical methods. Some examples include Fluid Dynamics and Finite Element Analysis. The grid, however, can be the source of great numerical uncertainty. Errors in simulations can arise from three sources, firstly, the input data, secondly, from approximations made to the model, and at last, from poorly refined grids (Paudel and Saenger, 2017). This last type of error cannot be avoided, nevertheless, it must be minimized so that a reliable solution can be obtained.

In general, hexahedral grids are associated with higher quality solutions, whereas a tetrahedral grid may increase numerical diffusion and therefore the uncertainty of the solution. The most commonly used method to assess grid convergence is the systematic grid refinement. However, this method alone is incapable of quantifying the uncertainties of the solution and therefore assess solution independence of the grid. The Grid Convergence Index (GCI) method is an established method of assessing grid convergence. It was developed based on the Richardson extrapolation with the objective of standardizing and giving more reliability to grid convergence results (Celik, 2008).

Several papers can be found in literature using the GCI method to assess grid convergence. Longest and Vinchurkar (2007) studied the grid convergence applying the GCI method to the deposition of particles in the respiratory tract, in which tetrahedral, hexahedral and hybrid grids were compared and systematically refined. Volk *et al.* (2017) performed a study on the grid convergence of the grid applied to a three-dimensional fixed bed model in a coupled CFD-DEM simulation, in this study, non-uniform and uniform refinements were done in several directions, with results indicating that the refinements must be performed systematically. Hodis *et al.* (2012) performed a study using the GCI to quantify the uncertainties related to grid convergence of a CFD model of a hemodynamic solution in aneurysm patients, this work emphasized the importance of estimating grid uncertainties.

Although many CFD work has been done concerning membranes, very little is reported when it comes to grid convergence applied to flow in membranes. Rahimi *et al*. (2009) in their study reported that the strategy used to assess grid convergence was to compare the solution results of each grid to those of experimental data, however, this practice does not guarantee that the errors due to numerical uncertainty are minimized to an acceptable level. Zhuang *et al*. (2017) performed a CFD study of a hollow fiber membrane module, in their work is mentioned the use of the GCI for assessing grid convergence, though, without more detail.

Therefore, the aim of this work was to quantify the uncertainties of grid convergence of a hollow fiber microfiltration membrane model in presence of concentration polarization using the GCI method. The model used in this work is based on studies performed by Damak (2004), Cunha (2014) and Souza (2014), in which the local permeation velocity is calculated using the resistance-in-series model.

2 GRID REFINEMENT STUDY

The procedure for grid refinement and uncertainty quantification outlined in this paper is originally proposed by Celik (2008). This procedure is based on the Richardson extrapolation, which relies on the assumption that any discrete solution has a series representation. The idea of this method is to give an estimate of the exact solution by extrapolating the solutions of the numerical grids.

The procedure proposed by Celik (2008) is composed of 5 steps. Initially, it was necessary to define the representative grid size h of each grid according to the equation (1).

$$h = \left[\frac{1}{N} \sum_{i=1}^{N} \left(\Delta V_i \right) \right]^{1/3} \tag{1}$$

In which ΔV_i is the volume of the i^{th} cell and N is the total number of cells in the grid. The volume is used in this case as the grid is three dimensional.

For the study, three different sets of grids were selected in a way that the refinement factor, defined by equation (2), was greater than 1.3.

$$r = \frac{h_{coarse}}{h_{refined}} \tag{2}$$

Other studies (Almohammadi *et al*,2013; Paudel and Saenger, 2017; Volk *et al*, 2017) point out that the refinement factor must be equal or greater than 2.0, therefore, this condition was satisfied in this study.

Let ϕ denote the solutions for a variable which can be considered key to the results, also let $h_1 < h_2 < h_3$, $r_{21} = \frac{h_2}{h_1}$, $r_{32} = \frac{h_3}{h_2}$. The apparent order p was calculated by equations (3), (4) and (5).

$$p = \frac{1}{\ln(r_{21})} \left| \ln \left| \frac{\varepsilon_{32}}{\varepsilon_{21}} \right| + q(p) \right| \tag{3}$$

$$q(p) = \ln \left(\frac{r_{21}^{p} - s}{r_{32}^{p} - s} \right) \tag{4}$$

$$s = sign \left(\frac{\varepsilon_{32}}{\varepsilon_{21}} \right) \tag{5}$$

where $\varepsilon_{32} = \phi_3 - \phi_2$, $\varepsilon_{21} = \phi_2 - \phi_1$, in which the number in the subscript denotes the solution of the respective grid, the subscript 1 refers to the finest grid, while the subscript 3 refers to the coarsest one. The solution of the equations (3), (4) and (5) requires the use of a fixed point iterative method with the initial guess equal to the first term of the equation (3). The function $sign$ in equation (5) will return a value of either 1 or -1. It must be highlighted that the value of $\frac{\varepsilon_{32}}{\varepsilon_{21}}$ is an indicator of oscillatory convergence, in a way that, if $\frac{\varepsilon_{32}}{\varepsilon_{21}} > 1$ then the point will have oscillatory convergence, if $0 < \frac{\varepsilon_{32}}{\varepsilon_{21}} < 1$ indicates the point will converge monotonically, and values of $\frac{\varepsilon_{32}}{\varepsilon_{21}} < 0$ indicate divergence (Paudel and Saenger, 2017).

The extrapolated values were calculated according to equation (6).

$$\phi_{ext}^{21} = \frac{(r_{21}^p \phi_1 - \phi_2)}{\left(r_{21}^p - 1\right)} \tag{6}$$

The approximate relative error was calculated according to the equation (7).

$$e_a^{21} = \left| \frac{\phi_1 - \phi_2}{\phi_1} \right| \tag{7}$$

Finally, the GCI was determined according to the equation (8).

$$GCI = \frac{1.25 e_a^{21}}{r_{21}^p - 1} \tag{8}$$

3 MATHEMATICAL MODEL

3.1 Problem description

The physical problem proposed consists of the tangential flow of fluid through a hollow fiber membrane. The hollow fiber has an effluent inlet and a concentrated outlet, while the filtrated fluid passes through the porous membrane wall, as is shown in “Fig. 1”. The hollow fiber membrane has the following dimensions: 200 mm in length, 1.55 mm of inner diameter and 0.3 mm of membrane thickness.

The domain of study of the present work is shown in “Fig. 2” and highlighted. Due to the axisymmetric behavior of the flow, a 20o cut of the internal cylinder was assumed. Also, it can be noticed that only the fluid region was covered, as the modelling of the porous part of the membrane was not necessary. Instead, a resistance-in-series model was adopted based on previous work done by Paris (2002), Damak (2004), Cunha (2014) and Souza (2014).

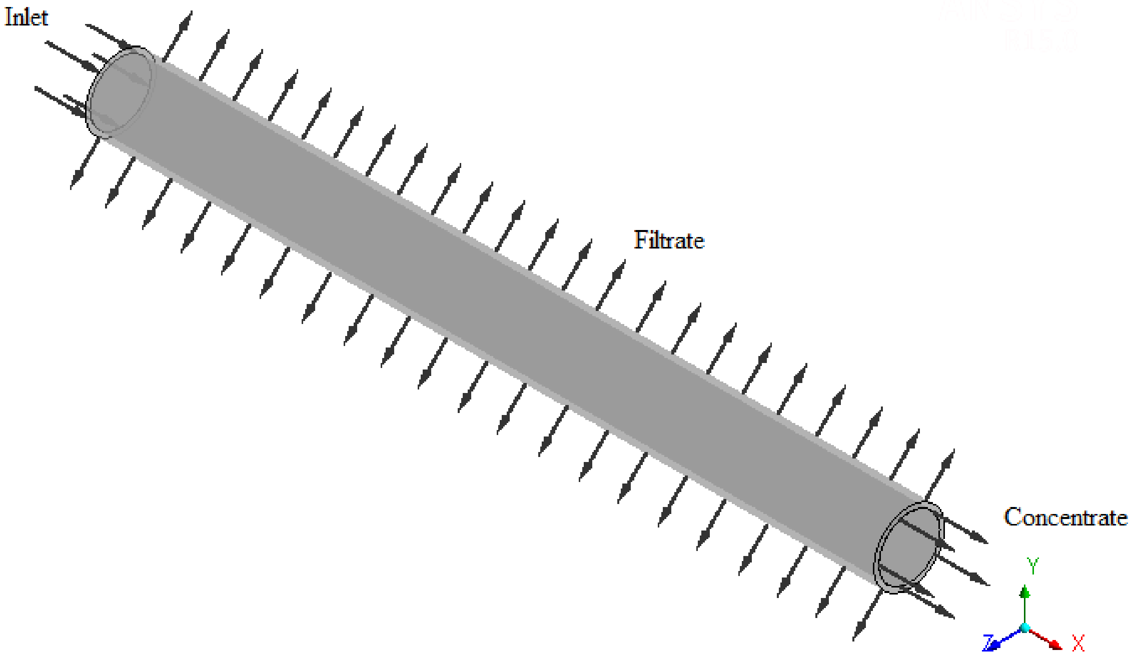

Figure 1. Scheme of the hollow fiber membrane with the fluid flow directions.

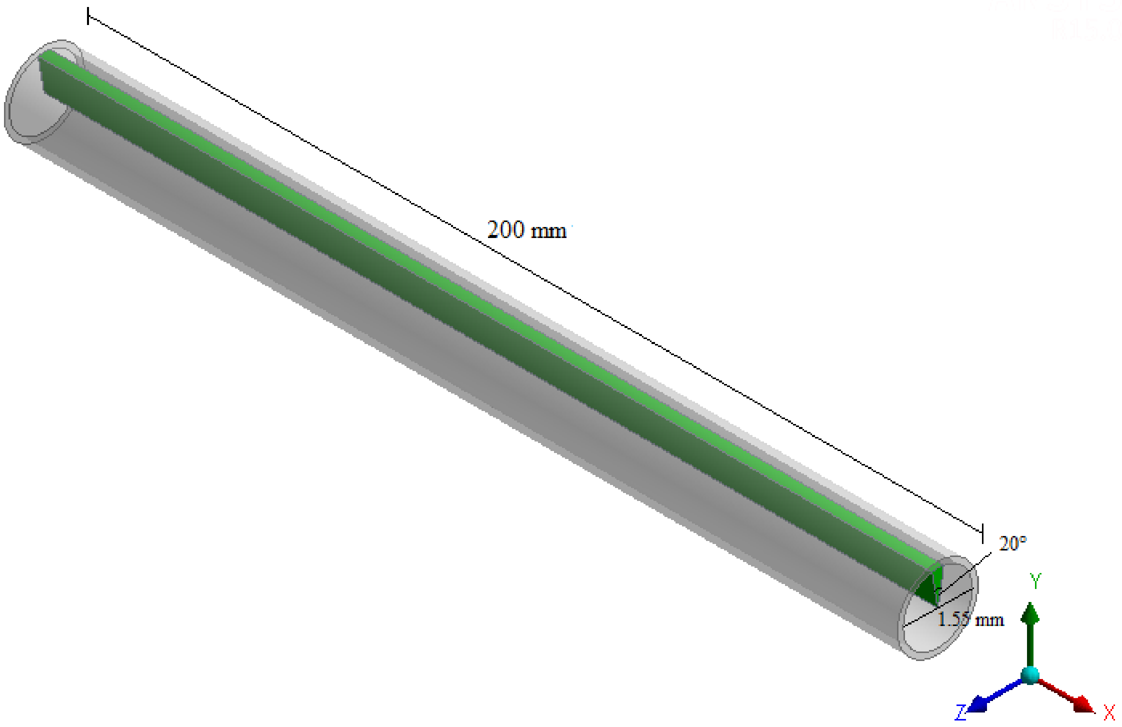

Figure 2. Detail of the domain of study.

3.2 Mathematical model

The mathematical model is a set of equations which represent the physical phenomena. In order to develop the equations, a set of assumptions is needed. In this work, the hollow fiber is considered to operate in a steady-state, in which the fluid dynamics equations were applied. Also, the following assumptions were also considered:

- Incompressible and laminar flow;
- solute particles are spherical and considered of same size;
- solute diffusion obeys the Stokes-Einstein law;
- gravity effects are neglected;
- wall permeation velocity is determined by the resistance-in-series theory and
- the concentration polarization layer is considered homogenously distributed, therefore the Kozeny-Carman equation is valid.

As is described in the proposed problem, the flow can then be described by the conservation of momentum and mass equations together with the conservation of species equation, which together, form a system of partial differential equations.

- Conservation of mass

$$\nabla \cdot (\rho \vec{U}) = 0 \tag{9}$$

- Conservation of momentum

$$\nabla \cdot (\rho \vec{U} \times \vec{U}) = -\nabla P + \nabla \cdot \mu \left(\nabla \vec{U} + (\nabla \vec{U})^T - \frac{2}{3} \delta \nabla \cdot \vec{U} \right) \tag{10}$$

- Conservation of species

$$\vec{U} \cdot \nabla C = D_{AB} \nabla^2 C \tag{11}$$

where P stands for pressure, μ is the dynamic viscosity of the fluid, δ is the identity matrix, C is the solute concentration and D_{AB} is the mass diffusion coefficient of the solute in water, which is determined by the Stokes-Einstein law and calculated through equation (12).

$$D_{AB} = \frac{k_B T}{6\pi\mu\varphi} \tag{12}$$

where k_B is the Boltzmann constant, T is the absolute temperature and φ is the radius of the spherical particles.

3.3 Boundary Conditions

For the solution of the differential equations of the model, the following boundaries conditions were defined; the boundaries are shown in “Figure 3”:

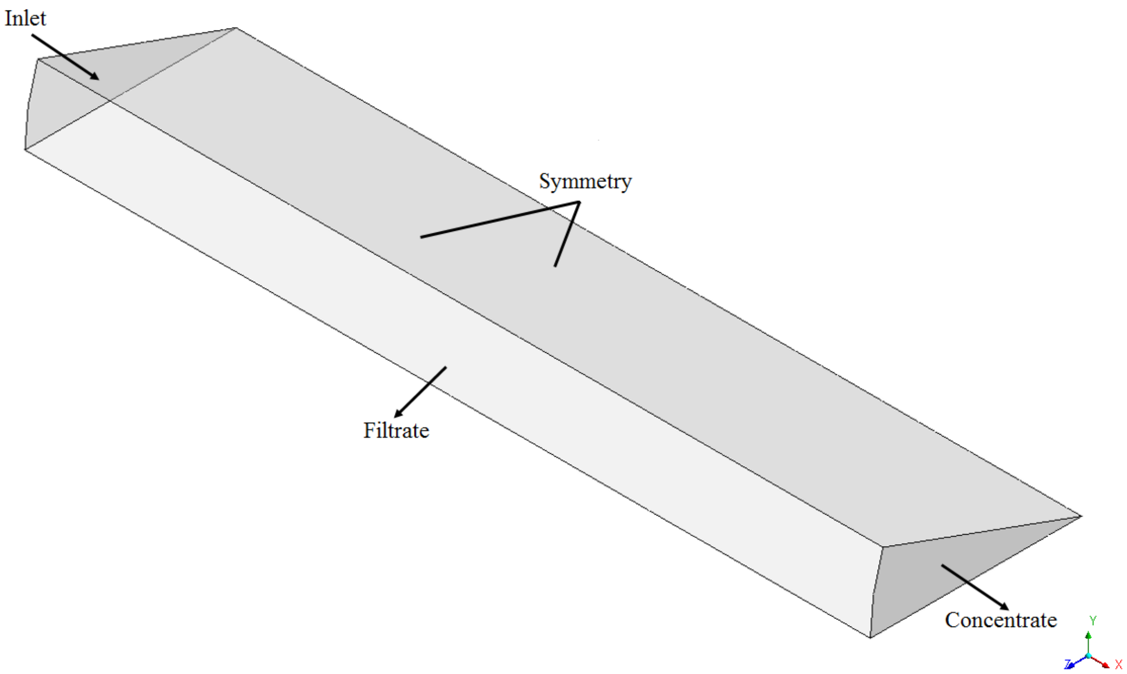

Figure 3. Boundaries of the domain of study.

3.3.1 Inlet

$$U_x = 2\overline{U_x}\left(1-\left(\frac{r}{R}\right)\right) \tag{13}$$

$$U_r = 0 \tag{14}$$

$$C = C_0 \tag{15}$$

Where r is the radial distance from the x-axis, R is the membrane inner radius and $\overline{U_x}$ is the maximum mean velocity in the x direction given by:

$$\overline{U_x} = \frac{\mathrm{Re}\,\mu}{\rho D} \tag{16}$$

In which Re is the Reynolds number and ρ is the fluid density.

Proceedings of the XXXVIII Iberian Latin-American Congress on Computational Methods in Engineering
P.O. Faria, R.H. Lopez, L.F.F. Miguel, W.J.S. Gomes, M. Noronha (Editores), ABMEC, Florianópolis, SC, Brazil, November 5-8, 2017.

3.3.2 Filtrate

$$U_x = 0 \tag{17}$$

$$U_r = \frac{\Delta P}{\mu\left(R_m + R_p\right)} \tag{18}$$

$$U_r C = D_{AB}\frac{\partial C}{\partial r} \tag{19}$$

where ΔP is the transmembrane pressure, R_m is the membrane resistance term, which can be calculated through equation (20), and R_p is the concentration polarization term, calculated through equation (21).

$$R_m = \frac{e}{\kappa} \tag{20}$$

where e is the membrane thickness and κ is the membrane permeability.

$$R_p = r_p \delta_p \tag{21}$$

Where r_p is the specific resistance due to concentration polarization, which was calculated through the Kozeny-Carman equation, given by equation (22), and δ_p is the concentration polarization layer thickness, calculated using equation (23).

$$r_p = 180\frac{\left(1-\varepsilon_p\right)^2}{d_p{}^2\varepsilon_p^3} \tag{22}$$

$$\frac{\delta_p}{D} = 2\left(\frac{x}{D}\right)^{0,33}\left(\mathrm{Re}\,Sc\right)^{-0,33}\mathrm{Re}_w^{-0,3}\left(1-0,4377Sc^{-0,0018}\,\mathrm{Re}_w^{-0,1551}\right) \tag{23}$$

Where ε_p is the concentration polarization layer porosity, d_p is the solute particle diameter, Re_w is the Reynolds number near the membrane wall, Sc is the Schmidt number which is calculated by equation (24).

$$Sc = \frac{\mu}{\rho D_{AB}} \tag{24}$$

3.3.3 Concentrate

The boundary condition at the concentrate outlet was assumed equal to atmospheric pressure ($P = 1\,atm$).

3.3.4 Symmetry

Due to the axisymmetric behavior of the flow in the interior of the membrane, symmetry condition was applied to the remaining boundaries of the domain.

3.4 Mesh generation and numerical procedures

The Ansys ICEM® software was used to produce the grid for the study, while the Ansys CFX® package was used to perform the simulations. A high-resolution advection scheme was used and a convergence criterion of 10^{-6} root mean square for all variables.

For the study, three grids were produced, with respectively 87759, 10863 and 1080 elements. Details of the grid are shown in "Figs. 4, 5, 6" and "7". It can be observed in the "Figs. 5, 6" and "7" that refinements were made in the X and Y directions, with finer elements closer to the inlet and the filtrate boundaries.

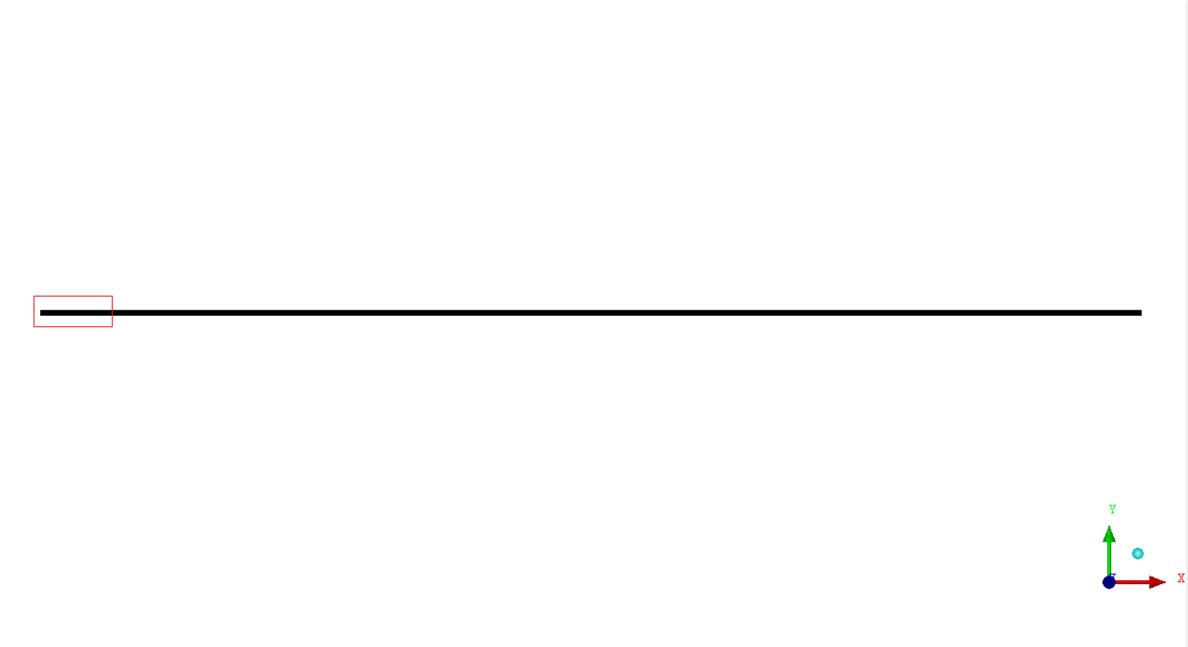

Figure 4. Region of the grid which is zoomed in subsequent figures.

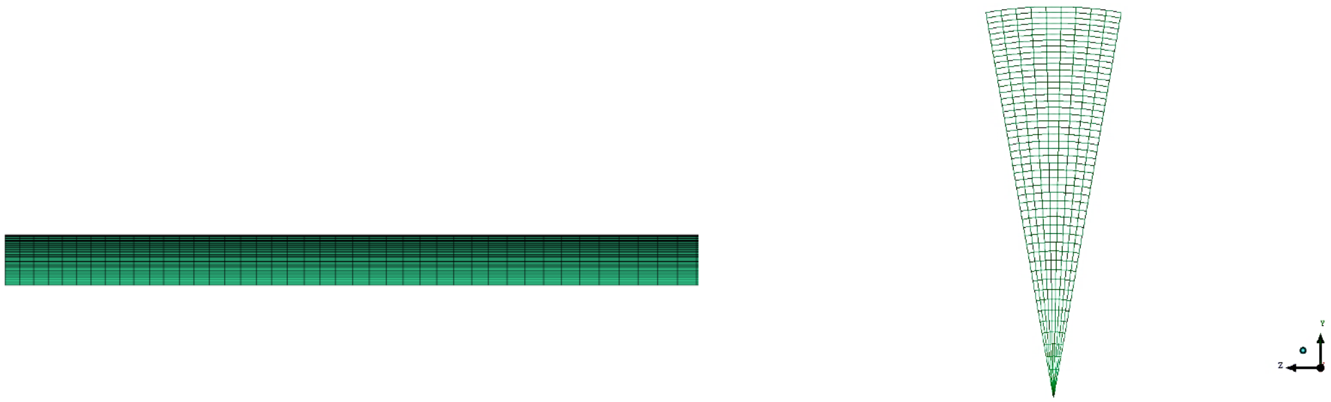

(a) (b)

Figure 5. Detail of the 87759 grid (a) side view close to inlet (b) frontal view.

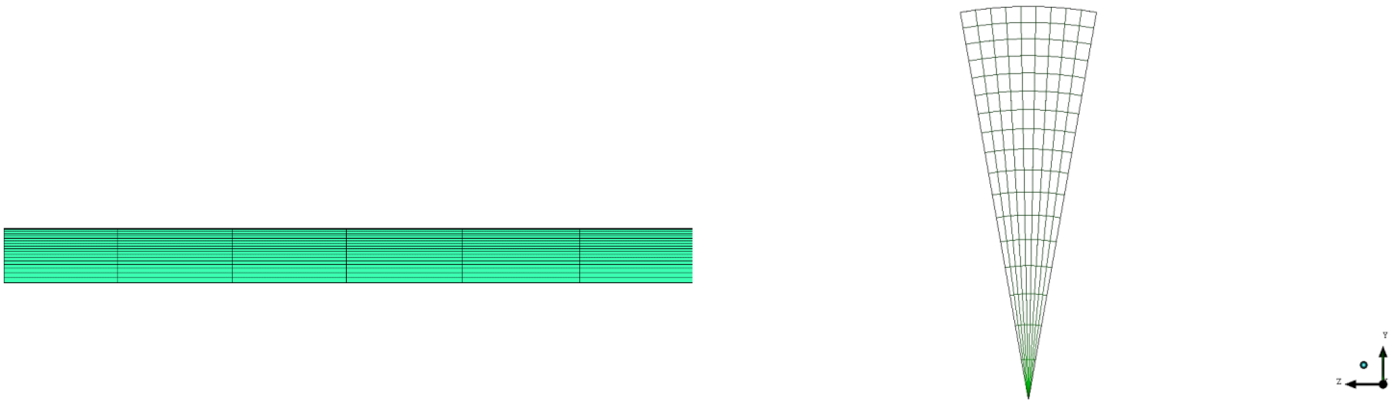

(c) (d)

Figure 6 Detail of the 10863 grid (a) side view close to inlet (b) frontal view.

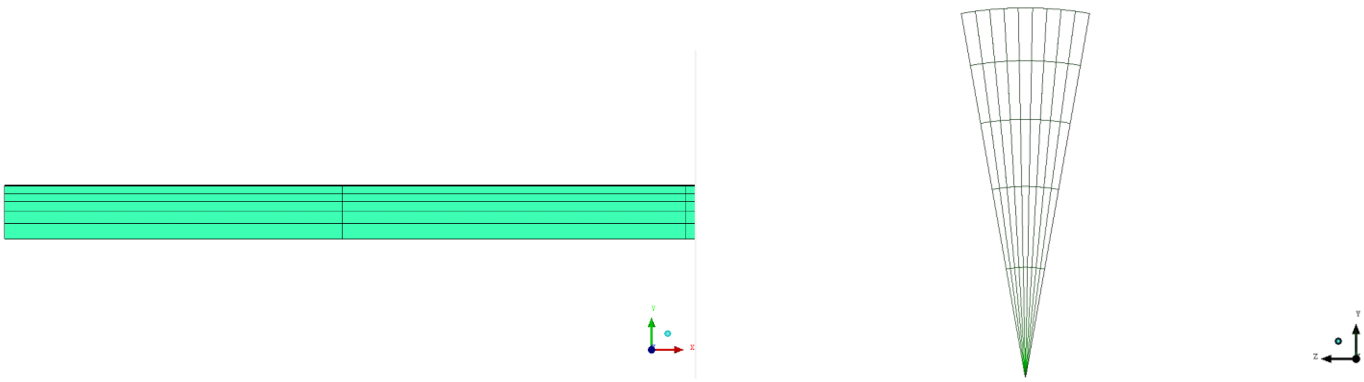

(e) (f)

Figure 7. Detail of the 1080 grid (a) side view close to inlet (b) frontal view.

4 RESULTS AND DISCUSSION

The grids were generated in the order from the coarsest to the finest grid. To apply the GCI method, it was necessary to guarantee that the grid refinement factors be close to 2 (Roache, 1994; Paudel and Saenger, 2017). The produced grids presented representative cell sizes of respectively 2.69e-4, $1.24 \cdot 10^{-5}$ and $6.21 \cdot 10^{-5}$ for the 1080, 10863 and 87759 grids respectively. The refinement factors are reported 2.00 for r_{21} and 2.15 for r_{32}.

"Fig. 8" presents the dimensionless velocity profiles of the flow at $x/H = 1.24 \cdot 10^{10}$, while "Fig. 9" presents the velocity profile's GCI of the finest grid at $x/H = 1.24 \cdot 10^{10}$ in the form of error bars. A p value of 3.28±0.71 was obtained. Monotonic convergence was achieved in 80% of the points, while only 20% of the points diverged, there was no points with oscillatory convergence.

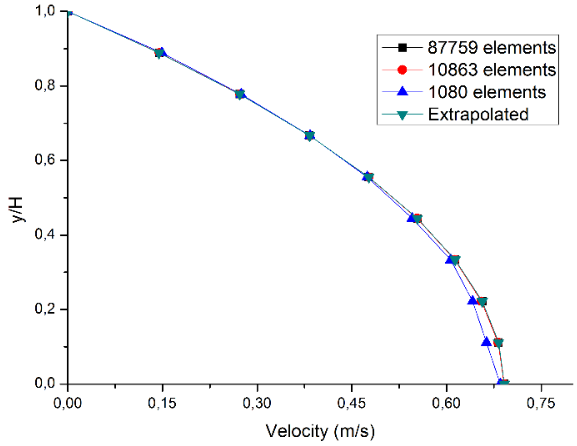

Figure 8. Velocity profiles of the flow at $x/H = 0.5$.

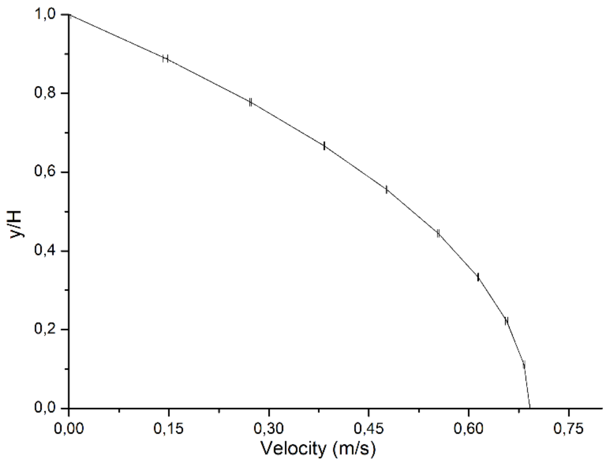

Figure 9. Velocity profile of the extrapolated grid with error bars at $x/H = 0.5$.

Analyzing "Fig. 8", it is noted that the solution of the extrapolated grid is very close to the finest grids, which is confirmed by the error bars in "Fig 9".

To assess the convergence of the grid, literature reports that the limit for the uncertainty for a grid to be considered converged is 10% (Chen and Thompson, 2002). For this variable, the maximum GCI was 0.046%, therefore, the grid with 87759 elements can be considered converged for the velocity at $x/H = 1.24 \cdot 10^{10}$.

"Fig. 10" presents the dimensionless concentration polarization layer thickness profiles for each grid, together with the calculated extrapolated grid solution, while "Fig. 11" presents the finest grid solution for the concentration polarization layer thickness profile with the uncertainty plotted in the form of error bars.

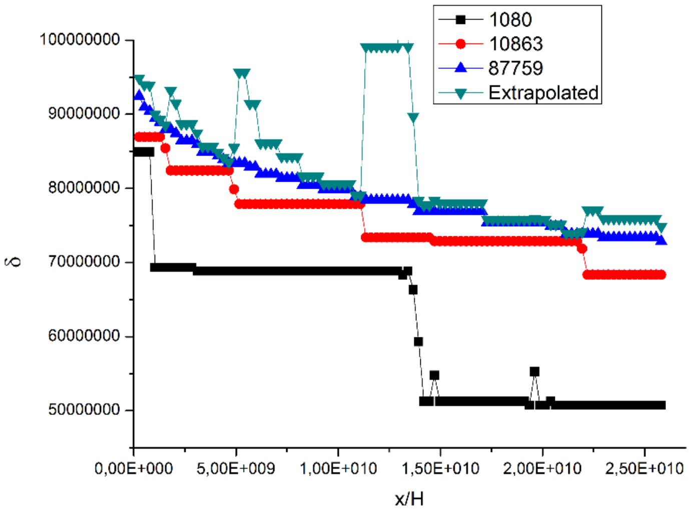

Figure 10. Concentration polarization layer thickness profiles.

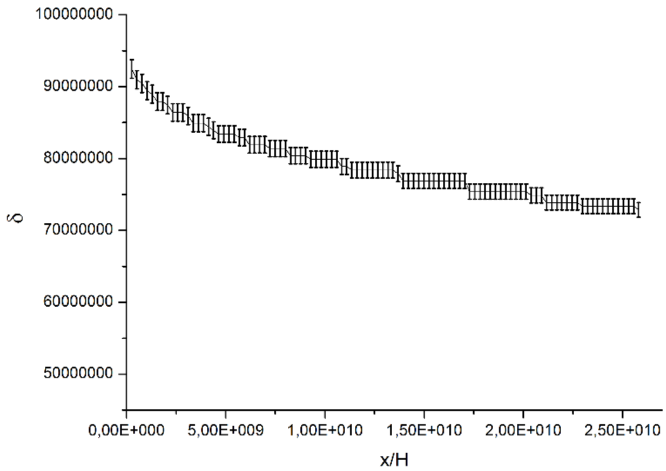

Figure 11. Concentration polarization layer thickness profile of the fine grid solution with error bars.

From "Fig. 9" it is possible to verify a gain in the quality of the solution from the coarsest to the finest grid. The discontinuity seen in the concentration profile of the grid with 1080 elements indicates a poor solution, this behavior is still present, though in a subtler way, in the grid with 10863 elements, however, the grid with 87759 elements does not present this behavior.

For the variable of solute concentration polarization layer thickness, the value of p was of 1.81±0.88, monotonic convergence was achieved in 100% of the points. The maximum value of the GCI for this variable was of 4.11%, therefore, the grid can be considered converged with 87759 elements.

5 CONCLUSION

The present work has proposed to use the GCI method to evaluate convergence of the grids of a model of the fluid flow through a hollow fiber membrane. A method for quantifying the uncertainties of the grids was presented based on the Richardson Extrapolation.

The results have shown that the GCI is a very efficient method for assessing grid convergence. It can not only indicate whether the results of a certain grid are reliable, but also quantitatively assess the uncertainties of the grid, and if it needs further refinement.

The results of this study have shown that, for the studied variables, which are relevant for the particular model implemented for the study, the grid with 87759 elements presented maximum levels of uncertainties of 0.048% for the velocity variable and 4.11% for the concentration thickness profile, which are considered acceptable by the literature.

ACKNOWLEDGEMENTS

The authors would like to gratefully acknowledge CAPES for partially supporting this work.

REFERENCES

Almohammadi, K. M., Ingham, D. B., Ma, L., Pourkashan, M., 2013. Computational Fluid Dynamics (CFD) mesh independency techniques for a straight blade vertical axis wind turbine. *Energy*, vol 58, pp. 483-493.

Celik, I. B., 2008. Procedure for Estimation and Reporting of Uncertainty Due to Discretization in CFD Applications. *Journal of Fluids Engineering*, v. 130, n. 7, pp 078001-1 – 078001-4

Chen, C. F. A., Lotz, R. D., Thompson, B. E., 2002. Assessment of uncertainty around shocks and corners on blunt trailing-edge supercritical airfoils. *Computers & Fluids*, vol. 31, issue 1, pp 25-40.

Cunha, A. D. L., 2014. *Tratamento de efluentes da indústria de petróleo via membranas cerâmicas – Modelagem e Simulação*. DSc Thesis, Universidade Federal de Campina Grande.

Damak, K., Ayadi, A., Schmitz, P., Zeghmati, B., 2004. Modeling of crossflow membrane separation processes under laminar flow conditions in tubular membrane. *Desalination*, vol. 168, n. 3, pp. 237-239.

Hodis, S., Uthamaraj, S., Smith., A. L., Dennis, K. D., Kallmes, D. F., Dragomir-Daescu, D., 2012. Grid convergence errors in hemodynamic solution of patient-specific cerebreal aneurysms. *Journal of Biomechanics*, vol. 45, n. 16, pp. 2907-2913.

Longest, P. W., Vinchurkar, S., 2007. Effects of mesh style and grid convergence on particle deposition in bifurcating airway models with comparisons to experimental data. *Medical Engineering & Physics*, vol. 29, n. 3, pp. 350-366.

Paris, J., Guichardon, P., Charbit, F., 2002. Transport phenomena in ultrafiltration: a new-two-dimensional model compared with classical models. *Journal of Membrane Science*, vol. 207, n. 1, pp. 43-58.

Paudel, S., Saenger, N., 2017. Grid refinement study for three dimensional cfd model involving incompressible free surface flow and rotating object. *Computers & Fluids*, vol. 143, pp. 134-140.

Rahimi, M., Madaeni, S. S., Abolhasani, M., Alsairafi, A. A., 2009. CFD and experimental studies of fouling of a microfiltration membrane. *Chemical Engineering and Processing: Process Intensification*, vol. 48, n. 9, pp. 1405-1413.

Roache, P. J., 1994. Perspective: A Method for Uniform Reporting of Grid Refinement Studies. *Journal of Fluids Engineering*, v. 116, n. 3, p. 405-413.

Souza, J. S. D., 2014. *Estudo teórico do processo de microfiltração em membranas cerâmicas*. DSc thesis, Universidade Federal de Campina Grande.

Volk, A., Ghia, U., Stoltz, C., 2017. Effect of grid size and refinement method on CFD-DEM solution trend with grid size. *Powder Technology*, vol. 311, pp. 137-146.

Zhuang, L., Guo, H., Dai, G., Xu, Z. L., 2017. Effect of the inlet manifold on the performance of a hollow fiber membrane module-A CFD study. *Journal of Membrane Science*, vol. 526, pp. 73-93.